Artifacts Reduction in Mutual Information-based Image Registration

Jundong Liu
School of Electrical Engineering
and Computer Science
Ohio University
Athens, OH 45701

Junhong Liu
Nokia Inc.
6000 Connection Drive
Irving, TX 75039

Abstract Mutual information (MI) is currently the most popular match metric in handling the registration problem for multi modality images. However, interpolation artifacts impose deteriorating effects to the accuracy and robustness of MI-based methods. This paper analyzes the generation mechanism of the artifacts inherent in partial volume interpolation (PVI) and shows that the mutual information resulted from PVI is a convex function within each voxel grid. A new joint entropy estimation scheme using prior information is proposed to reduce the artifact effects and we demonstrate the improvements via experiments on misalignments between MR brain scans obtained using different image acquisition protocols.

Keywords: Image Registration, Mutual Information, Artifacts Reduction

1 Introduction

Image registration is one of the most widely encountered problems in a variety of fields including but not limited to medical image analysis, remote sensing, satellite imaging, optical imaging etc. Broadly speaking, image registration methods can be classified into two classes [18], namely feature-based and direct methods.

1.1 Feature-Based Methods

Feature-based methods typically involve extracting features such as surfaces, ridges, landmark points etc., and then using a match metric to find a matching between them under a class of parameterized or more generally non-parameterized transformations.

In [6], Evans *et al.* developed a registration scheme based on approximating the 3D warp between the model and target image by a thin plate spline fitted to landmarks. Feldmar et al. [7] developed a novel surface to surface nonrigid registration scheme, using a local affine transformation. Maintz et al. [12] compared edge and ridge-based registration of CT and MR brain images. For more on feature-based methods, we refer the reader to the survey by Maintz et al. [13].

1.2 Direct Methods

Direct methods subsume the approaches operating directly on the image grey values, without prior feature extraction.

One straightforward intensity value based approach is the locally adaptive correlation window scheme [14]. A more general scheme than window-based correlation approach is the optical flow formulation, in which the problem of registering two images is treated as equivalent to computing the flow between the data sets. There are numerous techniques for computing the optical flow from a pair of images [8, 1, 5, 9] and we refer the reader to the survey by Barron *et al.* [1].

1.3 Image Similarity Measures

Another class of intensity value based approaches is based on statistical similarity measures.

Variance of Intensity Ratio is the first and simplest statistical measure proposed by Woods *et al.* [21] for registering PET and MRI images. Leventon *et al.* [10] proposed a method based on matching the *Joint Intensity Distribution* of current input image with the prior joint intensity distribution obtained from training data sets. Two methods are used to model the joint intensity distribution of the training data, mixture of Gaussians and Parzen windowing.

Currently the most popular approach is based on the concept of maximizing mutual information reported in Viola and Wells [19] and Wells *et al.* [20], Collignon *et al.* [3] and Studholme *et al.* [16]. For

two images, mutual information is a measure of how well one image explains the other, or vice versa. Although MI methods are regarded as the best choice for the multimodal image registration problem, a number of studies have pointed out that the robustness and accuracy of MI metric is deteriorated by the interpolation artifact effects. Several methods have proposed to address this problem [3, 15, 17, 11].

This paper is a further investigation of the artifacts problem. The generation mechanism of the artifact associated with the *partial volume interpolator*, which is regarded as the best choice among all possible interpolators, is analyzed and correspondingly, a new joint entropy estimation scheme using prior information is proposed to reduce the artifact effects. Experiment results using MR T1/T2 images are provided to demonstrate the improvements.

2 Mutual Information Metric and Artifact Effects

2.1 Mutual Information

Consider two images $I_r(x, y)$ and $I_f(x, y)$. We designate I_r as the reference image and I_f as the floating image. Registration is to find the coordinate transformation, denoted as T, such that transformed floating image $I_f(T(x, y))$ is aligned with the reference $I_r(x, y)$. The alignment is usually obtained by optimizing a certain similarity metric. So normally a registration algorithm consists of three components [1]: a coordinate transform, a similarity criteria, and a numerical scheme to seek the optimum.

Mutual information is currently the most popular matching metric being used in handling the registration problem for multimodal images. The MI between two discrete random variables, A and B, is defined as [4]:

$$MI(A, B) = \sum_{a,b} p_{AB}(a, b)\ log \frac{p_{AB}(a, b)}{p_A(a).p_B(b)} \qquad (1)$$

where $p_A(a)$, $p_B(b)$ and $p_{AB}(a, b)$ are the marginal probability distributions and joint probability distribution, respectively. The relationship between MI and entropy is:

$$MI(A, B) = H(A) + H(B) - H(A, B) \qquad (2)$$

with $H(A)$ and $H(B)$ being the entropy of A and B, and $H(A, B)$ their joint entropy.

$$\begin{aligned} H(A) &= -\textstyle\sum_a p_A(a)\ log\ p_A(a) \\ H(A, B) &= -\textstyle\sum_{a,b} p_{AB}(a, b)\ log\ p_{AB}(a, b) \end{aligned} \qquad (3)$$

Given a set of samples, there are several approaches to estimate the probability functions $p_{AB}(a, b)$, most notably the histogram-based method [3] and Parzen window method [19, 20]. In this paper, we focus on histogram-based method because it's widely used in image registration. To register the images the mutual information is to be maximized.

The advances of mutual information based methods reside not only in the impressive accuracy in the reported registration experiments, but also the generality the MI methods can provide. Very few assumptions ever made regarding the relationship that exists between the image intensities, so mutual information is especially suited for multi-modality matching and that it is completely automatic.

Studholme *et al.* [16] pointed out the standard mutual information is sensitive to the field of view of the scanner used in the image acquisition, namely, with different choices of field of view, the maximization process may lead to an incorrect alignment. The authors then extended the mutual information to a normalized mutual information to alleviate this problem:

$$NMI(A, B) = (H(A) + H(B))/H(A, B) \qquad (4)$$

2.2 Interpolation Artifact Effects

For digital images $I_r(x, y)$ and $I_f(x, y)$ to be aligned, interpolation is necessary to evaluate the values of $MI(I_r(x, y), I_f(T(x, y))$. A number of interpolators are available, including nearest neighbor (NN), linear, cubic spline, Hamanning-windowed sinc and partial volume (PV) interpolators. Among them, PV is regarded as the best choice for MI-based metrics, as pointed out by several studies [17, 12].

Partial volume interpolation is not an interpolation in the ordinary sense. It is a strategy being used to update the joint histogram. As shown in Figure 1, instead of interpolating the new intensity value under current transformation T, PV directly updates the histogram of the nearest neighbor bins with the same weights used in bilinear (for 2D) or trilinear (for 3D) interpolation.

In [15], Maintz *et al.* qualitatively explained the reason why artifacts are generated in partial volume interpolation process and verified their arguments through several well-designed experiments. While their work is very informative, we believe that a theoretically quantitative analysis concerning the generation mechanism of artifacts will be more instructive to guide the related research.

As interpolation affects the registration function of normalized MI and traditional MI in a similar way

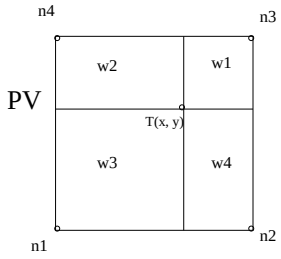

(a)

Figure 1: PV interpolation.

[15], we will construct our arguments based on traditional MI in this paper, but it should be noted that the conclusions also hold for normalized MI.

As given above, the mutual information $MI(A, T(B))$ consists of 3 terms: $H(A)$, $H(B)$ and $H(A, T(B))$. $H(A)$ is a constant. The computation of $H(T(B))$ is also affected by the interpolation effect, but in a much smaller extent. Figure 2 shows a pair of aligned MR/CT images and the associated marginal entropies, joint entropy and MI values as functions of translations up to ± 7 pixel distances. As evident, the variation of MI is dominated by the changes in $H(A, T(B))$; $H(A)$ and $H(T(B))$ are close to constants. So from now on, we will focus only on $H(A, T(B))$.

Let's first consider the situation where the reference and floating images have exactly the same pixel sizes and the motion is limited to translations only. We use the CT image in Figure 2 as the reference, while MR is the floating image. Now let's analyze the variation of MI function between the two images when the floating image moves from the alignment position to 1 pixel away along x axis.

Suppose at the alignment position (translation is equal to zero), a certain histogram bin $his(a, b)$ has a value of M_1. $his(a, b)$ records the total number of pixels in the image pair where the reference image has intensity a, and floating image b. Suppose when the translation is 1 pixel, $his(a, b)$ becomes M_2. Let's re-define the $his(a, b)$ to $his(a, b, t)$ to include the translation variable, then $his(a, b, 0) = M_1$ and $his(a, b, 1) = M_2$. In between, with the translation being t, there are a group of intensity grids $X1 = \{(x_1, y_1), (x_2, y_2)...\}$ that were originally contributing to the bin $his(a, b)$, gradually wipe out their support when the floating image is moving. Let's call this group of grids as the moving-out set, and let A_1 be the total number of these grids. Because the motion here is limited to translation only, all the grids in the moving-out set are withdrawing their contributions to the bin $his(a, b)$ at the same rate, as the translation increases from 0 to 1. When the translation is 0, each of them contribute an $'1'$ to $his(a, b)$; when the offset is 1, they do not have contribution any more. In between, the contribution of the each moving-out grid is $1 - t$.

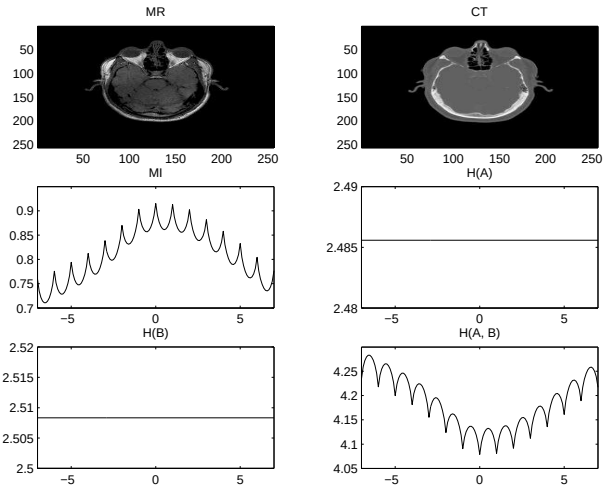

(a)

Figure 2: The mutual information value of a pair of multimodal images. Row 1 contains a pair of MR/CT images. Row 2 and row 3 shows the mutual information(MI),marginal entropies ($H(A)$ and $H(T(B))$) and joint entropy ($(HA, T(B))$) values as functions of translations t (up to ± 7 pixels).

Similarly, there might be another group of grids X_2 (let A2 be the total number) that were not originally contributing to $his(a, b)$, start moving in to contribute to $his(a, b)$ as the translation increases from 0 to 1. Their individual contribution to $his(a, b)$ is $'t'$ at translation t.

Overall, the combined effects of the moving-in and moving-out sets lead to the change of $his(a, b)$. So we have:

$$A_2 - A_1 = M_2 - M1; \tag{5}$$

At translation t:

$$\begin{aligned} his(a, b, t) &= M_1 + A_2\ t - A_1\ t \\ &= M_1 + (M2 - M1)\ t \\ &= t\ M_2 + (1 - t)\ M_1 \end{aligned} \tag{6}$$

So basically within interval $[0, 1]$, the bin value $his(a, b, t)$ is a linear function of the offset variable t,

denoted here by $f(t)$:

$$\begin{array}{l} f(0) = M1, \quad f(1) = M2 \\ f(t) = t\ f(1) + (1-t)\ f(0). \end{array} \tag{7}$$

Since we use histogram to approximate distribution, the joint entropy of two images can be rewritten as $H(A, T(B)) = -\sum_{a,b} his(a,b,t)\ log\ his(a,b,t)$. As we know, the function $x\ log\ x$, denoted by $g(x)$ here, is a convex function within the interval (0, 1] (note its second derivative is positive), i.e.:

$$g(t\ x_1 + (1-t)\ x_2) \leq t\ g(x_1) + (1-t)\ g(x_2)$$

Therefore, the individual contribution of the bin $his(a,b,t)$ to the joint entropy $H(A, T(B))$ follows:

$$\begin{array}{rcl} g(f(t)) & = & g((1-t)\ f(0) + t\ f(1)) \\ & \leq & (1-t)\ g(f(0)) + t\ g(f(1)) \end{array} \tag{8}$$

The inequality above indicates that each component of $H(A, T(B))$ is a convex function within $[0, 1]$. Since the summation of convex functions is still a convex function, $\mathbf{H(A, T(B)) = -\sum\sum g(his(a, b, t))}$, **as a negative combination of certain number of convex functions, is a concave function in** $[0, 1]$**. Correspondingly, the MI responses is a convex function in the same interval**. This property can be easily extended the any intervals $[n, n+1]$ where n is an integer. That's the reason the responses of $H(A, T(B))$ as a function of translation t (Figure 2) bears a concave-shaped artifact within each integer interval.

If we take a closer look at the above analysis, we can find that the heart of the artifact generation mechanism lies in the following fact: all the moving-in and moving-out grids contribute to the change of the bin value at a synchronized pace. As a consequence, a general guideline to reduce the artifact effects can be "to break the synchronization".

In addition, the following prediction can be made based on the above analysis:

- The artifact effect for pure rotations would be less severe than that of pure translations. This is because the moving-in and moving-out grids, under the pure rotation motion scenario, do not contribute to the change of histogram in a uniformly rate. Figure 3.a. shows the $H(A, T(B))$ values as a function for rotations (up to $\pm 15°$). As evident, the responses for rotations are much smoother than the translation counterpart.

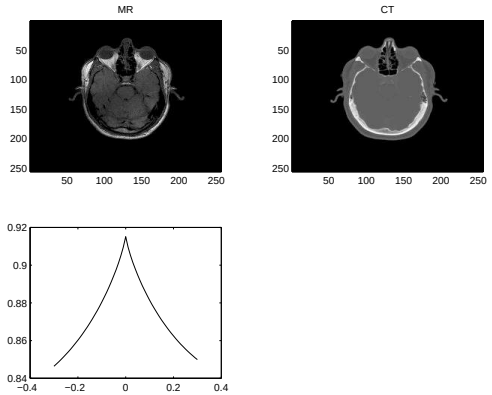

(a)

Figure 3: Row 1 contains a pair of MR/CT images. Row 2 shows the mutual information (MI) value as a function to rotaions ($\pm 20°$).

2.3 Artifacts Reduction

Based on the abolve analysis, we propose the an artifact effects reduction scheme based on integrating prior information. The idea is to wipe out the concave function portion of the joint entropy, with the linear function part kept. This task can be mostly done by combining the joint entropy $H(A, T(B))$ with a prior joint entropy $H^*(A, T(B))$. The justification is based on the assumption that the training data would provide a prior joint probability that is similar to the probability of the test data, therefore the artifact part can be effectively removed by subtracting the concave function part of the prior joint entropy. To achieve this end, we replace the MI metric with a modified version: $\bar{M}I(A, T(B)) = H(A) + H(T(B)) - (\bar{H}(A, T(B))$

Suppose T is a 2D rigid transform vector $\{\alpha, dx, dy\}$, let

$$\begin{array}{l} T_{00} = \{\alpha, floor(dx), floor(dy)\} \\ T_{01} = \{\alpha, floor(dx), ceil(dy)\} \\ T_{10} = \{\alpha, ceil(dx), floor(dy)\} \\ T_{11} = \{\alpha, ceil(dx), ceil(dy)\}, \end{array}$$

where $floor$ and $ceil$ stand for floor and ceiling operations respectively. The modified joint entropy $\bar{H}(A, T(B))$ is defined as follows:

$$\begin{array}{l} \bar{H}(A, T(B)) = H(A, T(B)) - H^*(A, T(B)) \\ \quad + \quad BiLinear(H^*(A, T_{00}(B)), H^*(A, T_{01}(B)), \\ \qquad\qquad H^*(A, T_{10}(B)), H^*(A, T_{11}(B))), \end{array}$$

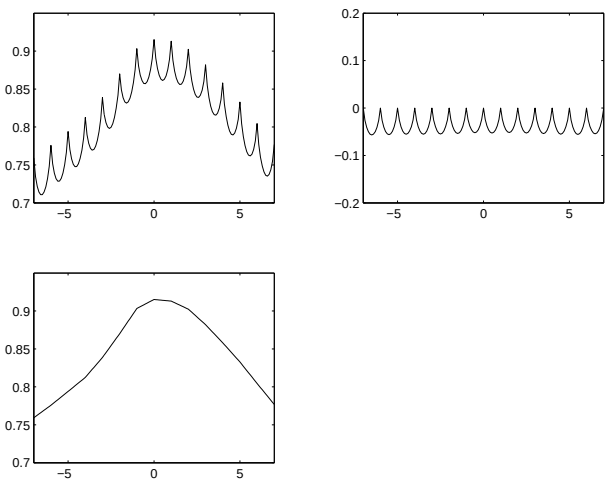

(a)

Figure 4: Top left: The MI artifact patterns for the CT/MR image pair. Top right: The prior concave function to be subtracted. Bottom left: $\bar{MI}$ responses after substracting the prior concave function.

where *BiLinear* is the bilinear interpolation operation.

Figure 4 depicts the registration for the new MI function. The top left subfigure of Figure 4 shows the MI artifact patterns for the CT/MR test image. The top right shows the concave function that is obtained from a pair of registered training images. As evident in the bottom subfigure, a significant reduction of interpolation artifacts was achieved after subtracting the concave function.

3 Experiment Results

In this section, we demonstrate the robustness property of the new MI computation method proposed in the previous section. All the examples contain synthesized miss-alignments applied to MR data sets from the brainweb site at the Montreal Neurological Institute [2].

The experiments are designed as follows: with a 2D MR T1 slice as the reference image, the floating image is obtained by applying a rigid transformation to a previously aligned 2D MR T2 image.

With 15 randomly generated rigid transformations, we applied our **Integrating Prior Joint Entropy** algorithms together with the traditional MI method to estimate motion parameters. These transformations are normally distributed around the values of $(0°, 10pixel, 10pixel)$, with standard deviations of $(5°,\ 3pixel\ 3pixel)$ for rotation and translation in x and y respectively.

Table 1 depicts the mean and standard deviation of the estimation errors obtained from the 2 methods. In each cell, the leftmost value is the rotation angle (in degrees), while the right two values show the translations in x and y directions respectively. Out of the 15 trials, the traditional MI failed 5 times while the **Integrating Prior Joint Entropy** never failed ("failed" here means that the results had unacceptably large errors). If we only count the cases which gave reasonable results, as shown in the first (for **Integrating Prior Joint Entropy**) and third (for traditional MI) rows, our approach and the traditional MI have comparable performances, all being very accurate. Note that Powells method was used as the optimization scheme in these experiments.

	mean			standard deviation		
1	$0.132°$	0.293	0.372	$0.012°$	0.112	0.230
2	$0.087°$	0.293	0.383	$0.031°$	0.121	0.129

Table 1: Comparison of estimation errors for rigid motion between Integrating Prior Joint Entropy and traditional MI.

4 Conclusions

In this paper, we quantitatively analyzed the generation mechanism of the interpolation artifacts. A new joint entropy estimation scheme using prior information is proposed to reduce the artifact effects. Comparisons were made between the traditional MI and the new method. Experimental results depicted better performance of using the modified method over the traditional MI.

Acknowledgments

We thank the brainweb data source creators at the Montreal Neurological Institute for the data.

References

[1] J. L. Barron, D. J. Fleet, and S. S. Beauchemin, "Performance of Optical Flow Techniques," *Intl. J. Comput. Vision*, 1(12):43-77,1994.

[2] Simulated brain database [Online]. Available : http://www.bic.mni.mcgill.ca/brainweb/

[3] A. Collignon, F. Maes, D. Delaere, D. Vandermeulen, and P. S. ang G. Marchal, "Automated multimodality image registration using information theory," *Proc. IPMI*,Y.J.C.Bizais, Ed., pp. 263-274,1995.

[4] Thomas M. Cover, Joy A. Thomas, *Elements of Information Theory,* John Wiley and Sons, 1991.

[5] J. H. Duncan and T. C. Chou (1992) "On the Detection of Motion and the Computation of Optical Flow," *IEEE Transactions on Pattern Analysis and Machine Intelligence*, 14(3):346-352, 1992.

[6] A. C. Evans, [1991], "Warping of Computerized 3D Atlas to Match Brain Image Volumes for Quantitative Neuroanatomical and Functional Analysis," *Proc. SPIE Medical Imaging V*, vol. 1445, pp. 236-246, 1991.

[7] J. Feldmar and N. Ayache, "Locally Affine Registration of Free-form Surfaces," *Proc. of IEEE CVPR*, pp. 496-501, Seattle, WA, 1994.

[8] Fleet, D.J. and Jepson, A.D., [1990], "Computation of Component Image Velocity from Local Phase Information," IJCV, Vol. 5, No.1 pp. 77-104.

[9] S. Gupta and J. Prince, (1995) "On Variable Brightness Optical Flow for Tagged MRI," *Proc. of IPMI*, pp. 323-334, Dordredcht, Kluwer, 1995.

[10] M. Leventon and W. E. L. Grimson, "Multi-modal volume registration using joint intensity distributions," in MICCAI 1999.

[11] B. Likar and F. Pernus, "A hierachical approach to elastic registration based on mutual information", *Image and Vision Computing*, 19, 2001, pp. 33-44.

[12] J. B. A. Maintz, P. A. van den Elsen and M. A. Viergever, "Comparison of Edge-based and Ridge-based Registration of CT and MR brain images," *Medical Image Analysis*, 1(2), pp. 151-161, 1996.

[13] J.B. Maintz and M. A. Viergever, "A Survey of Medical Image Registration," *MedIA* Vol. 2, pp. 1-36,1998.

[14] M. Okuomi and T. Kanade, (1992) "A Locally Adaptive Window for Signal Matching," *International Journal of Computer Vision*, 7(2), pp. 143-162, 1992.

[15] J. Pluim, J. Maintz and M. Viergever, "Interpolatioin artefacts in mutual information-based image registration," *Computer Vis Image Underst*, vol. 77, pp 211-232, 2000.

[16] C. Studholme, D. Hill and D. Hawkes, "An overlap invariant entropy measure of 3D medical image alignment," *Pattern Recognition*, Vol. 32, pp. 71-86,1999

[17] X. Ji, H. Pan and Z.P. Liang, "A region-based mutual information method for image registration", Proc. 7th Intl. Soc. Magn. Reson. Med., vol 3, pp 2193, May, 1999.

[18] B. C. Vemuri, S. Huang, et.a.l., "An efficient motion estimator with application to medical imaging," Med. Image Anal., 2(1), pp. 79-98, 1998.

[19] P. A. Viola and W. M. Wells, "Alignment by maximization of mutual information," in *Fifth ICCV*, MIT, Cambridge, MA, pp. 16-23, 1995

[20] W. M. Wells III, P. Viola, and H. Atsumi, "Multimodal Volume Registration by Maximization of Mutual Information," *Medical Image Analysis*, 1(1), pp. 35-51, 1997.

[21] R. Woods, J. Maziotta and S. Cherry "MRI-PET registration with automated algorithm," *J. Comput. Assis. Tomogr.*, 17, pp. 536-546, 1993.